Journal Pre-proof

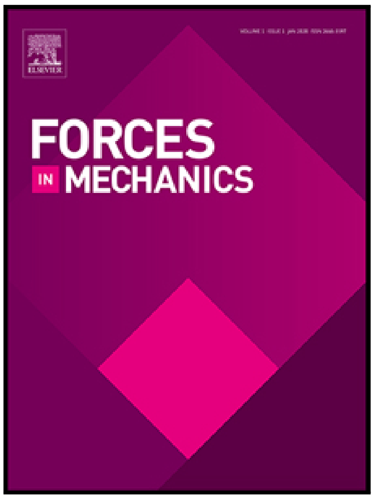

Modelling of the fatigue strength degradation due to a semi-elliptical flaw

Slobodanka Boljanović , Andrea Carpinteri

PII: S2666-3597(21)00011-1
DOI: https://doi.org/10.1016/j.finmec.2021.100020
Reference: FINMEC 100020

To appear in: *Forces in Mechanics*

Received date: 26 February 2021
Revised date: 1 April 2021
Accepted date: 3 April 2021

Please cite this article as: Slobodanka Boljanović , Andrea Carpinteri , Modelling of the fatigue strength degradation due to a semi-elliptical flaw, *Forces in Mechanics* (2021), doi: https://doi.org/10.1016/j.finmec.2021.100020

Highlights

- The performances of surface flaws are evaluated through a computational strategy under cyclic loading.
- Driving mode analysis, performed via novel analytical solutions, is verified using experimental observations.
- Through the fatigue life and crack path evaluations the crack shape effect is examined.

Modelling of the fatigue strength degradation due to a semi-elliptical flaw

Slobodanka Boljanović[1,*], Andrea Carpinteri[2]

[1] Mathematical Institute of the Serbian Academy of Sciences and Arts, Kneza Mihaila 36, Belgrade, Serbia, e-mail: slobodanka.boljanovic@gmail.com

[2] University of Parma, Department of Engineering and Architecture, Parco Area delle Scienze 181/A, Parma, Italy, e-mail: andrea.carpinteri@unipr.it

[*] Corresponding author; phone: +381 63 805 60 85, fax: +381 11 35 11 282

Abstract

Due to the fulfilment of modern operational requirements and time-consuming of complex fatigue responses computation, the surface micro-flaw analysis in large moving systems is still one of the challenging tasks. Thus, the present research work discusses the fatigue computational design strategy that can be used to properly evaluate the driving mode caused by a surface semi-elliptical flaw. Further, through the novel analytical solutions, experimentally assessed, the residual life and crack path are designed taking into account the crack shape effect.

Keywords: Driving mode, Fatigue response, Residual life, Semi-elliptical flaw

Nomenclature

a, b	crack length in depth/surface direction
C_A, C_B	material constants in fatigue crack growth law
da/dN	crack growth rate in depth direction
db/dN	crack growth rate in surface direction
E	elastic modulus
f_w	correction factor related to the plate width
f_ϕ	correction factor related to the location angle
g	correction factor for semi-elliptical surface crack
m_A, m_B	material constants in fatigue crack growth law
M_1, M_2, M_3	corrective factors for front-face, crack shape and crack size
N	number of loading cycles to failure
Q	ellipse shape factor
R	load/stress ratio
K	stress intensity factor
S	applied stress
t	thickness
w	width
ΔK	stress intensity factor range
ΔP	applied force range
ΔS	applied stress range

β, β_1	material fatigue parameters
ϕ	location angle
ν	Poisson's ratio

Subscripts

A	depth position
B	surface position
f	failure
max	maximum value related to the applied load
0	initial

1. Introduction

Sustainability, according to damage-tolerance philosophy, requires the protection of large moving systems from any kind of deterioration over their life cycle. However, sudden localized surface damages/defects due to complex loading profiles can seriously jeopardize the strength resource during exploitation. Thus, in order to avoid the detrimental effects of stress raiser in the safety critical spots, it is essential to develop reliable computational design strategies for evaluating the performances of quarter-elliptical and/or semi-elliptical crack-like flaws.

Micro-flaw phenomenon as one of key factors with respect to fatigue-induced hazard presents an important issue through several fracture mechanics-based research studies available in the literature. In this context, Jones et al. [1] have generated relevant solutions for assessing the stability of semi-elliptical flaws by means of the weight function method and the CTOD concept. The same surface stress raisers have been analyzed by Yamashita et al. [2] via the Paris' crack growth concept and the finite element method.

Furthermore, in order to explore the fatigue response of quarter-elliptical crack at pin-loaded hole, Antoni and Gaisne [3] have developed an analytical strategy. Then, Mikheevskiy et al. [4] have combined the UniGrow software code (based on the Noroozi et al. concept [5]) together with the weight function method. Boljanović et al. [6] have suggested that the same pin-loaded configuration can be analyzed employing the two parameter driving force model proposed by Kujawski [7] and the finite element method. By performing safety relevant assessment, Boljanović et al. [8] have also demonstrated that the performance of such a linkage can be successfully evaluated via Zhan et al. crack growth concept [9] together with the *J*-integral method.

Through the failure analysis of a semi-elliptical crack or a quarter-elliptical corner crack located at the edge notch, Newman et al. [10] and Wu et al. [11] have taken into account the crack closure concept, the weight function method and the finite element method. Later, Boljanović and Capinteri [12] have used the stress ratio-dependent crack growth concept [13] and the finite element method for evaluating the stress raising power of the same notch with a semi-elliptical flaw.

The present research work proposes a damage tolerance-based computational design code in order to gain insight on fatigue performance of surface micro flaws as well as on their potential to endanger the durability of plate-type configurations. In the frame of such an analytical strategy, the semi-elliptical crack advance modelling includes the cycle-by-cycle evaluations of the stress intensities and crack growth rates. Furthermore, relevant experiments from the literature demonstrate that this research study adds new insights into the detrimental mechanisms of flaws, and also provides a reference point for establishing a practical guideline that leads to further improvements in safety and cost reduction.

2. Pre-existing flaw growth under cyclic loading

The performance of a failure-relevant surface flaw is theoretically examined by employing the extended Huang-Moan crack growth concept [13], expressed as follows:

$$\frac{da}{dN}=C_A\left(M\,\Delta K_A\right)^{m_A} \qquad \frac{db}{dN}=C_B\left(M\,\Delta K_B\right)^{m_B} \tag{1}$$

where *da/dN* and *db/dN* are the crack growth rate in depth and surface direction, respectively, C_A, C_B, m_A, m_B represent material parameters experimentally obtained, and ΔK_A, ΔK_B are the stress intensity factors for two critical crack growth directions, mentioned above.

Through the fatigue vulnerability analysis of pre-existing flaws (Fig. 1) that can seriously jeopardize the structural integrity due to load-environment interactions, the following fracture mechanics-based parameter [13] is herein proposed:

$$M=\begin{cases}(1-R)^{-\beta_1} & -5\le R<0\\ (1-R)^{-\beta} & 0\le R<0.5\\ \left(1.05-1.4R+0.6R^2\right)^{-\beta} & 0.5\le R<1\end{cases} \tag{2}$$

where R is the stress ratio, and (β, β_1) are material parameters by which the time-variant load effects are taken into account.

Furthermore, relevant solutions for driving mode extension (see Eq. (1)) are employed to evaluate the strength degradation in terms of number N of loading cycles, from initial a_0, b_0 to final a_f, b_f crack length in depth and surface direction, respectively, i.e.

$$N=\int_{a_0}^{a_f}\frac{da}{C_A\left(M\,\Delta K_A\right)^{m_A}} \qquad N=\int_{b_0}^{b_f}\frac{db}{C_B\left(M\,\Delta K_B\right)^{m_B}} \tag{3}$$

Fracture mechanics-based design and preventive maintenance are an accepted practice in engineering to preserve the reliability of large moving systems at the highest possible level. Thus, a novel computational design code is here developed (in which the Euler's algorithm is used to compute the complex-valued functions) that provides a physical interpretation of the safety-relevant surface flaw progression.

PLEASE insert Figure 1 here.

3. Analysis of mode intensities in the vicinity of a semi-elliptical flaw

The durability of large moving systems is dependent on their responses to the actual in-service load profiles. Thus, an adequate knowledge of the driving force impacts in failure relevant spots is a prerequisite that must be achieved by using analytical and/or numerical strategies [3, 4, 6, 8, 14-19]. Through the present research work, the stability of a semi-elliptical flaw (Fig. 1) is explored applying the following fracture mechanics-based solution [20, 21]:

$$\Delta K = F_{\mathrm{sec}} \Delta S \sqrt{\frac{\pi a}{Q}} \tag{4}$$

where ΔS and a are applied stress range and crack length in depth direction, respectively, ΔK is the stress intensity factor range, and Q represents the ellipse shape factor.

Fatigue-induced stress state in the vicinity of micro-flaws characterized by $a/b \leq 1$ [20] is herein quantified by taking into account the crack-like flaw shape together with the applied load via the correction factor F_{sec}, expressed as follows:

$$F_{\mathrm{sec}} = \left(M_1 + M_2 \left(\frac{a}{t} \right)^2 + M_3 \left(\frac{a}{t} \right)^4 \right) g \, f_\phi \, f_w \tag{5}$$

$$M_1 = 1.13 - \frac{0.09\, a}{b} \tag{6}$$

$$M_2 = -0.54 + \frac{0.89}{0.2 + \frac{a}{b}} \tag{7}$$

$$M_3 = 0.5 - \frac{1}{0.65 + \frac{a}{b}} \tag{8}$$

$$g = \left(0.1 + 0.35\left(\frac{a}{t}\right)^2\right)(1 - \sin\phi) \tag{9}$$

where t is thickness of the plate, b and ϕ are crack length in surface direction and angle location on the crack front, respectively.

Further, through a driving mode analysis, the relevant correction factors Q, f_ϕ and f_w are employed to generate the effect of ellipse crack shape, location angle ϕ and the plate width w, respectively:

$$Q = 1 + 1.464\left(\frac{a}{b}\right)^{1.65} \tag{10}$$

$$f_\phi = \left(\left(\frac{a}{b}\right)^2 \cos^2\phi + \sin^2\phi\right)^{0.25} \tag{11}$$

$$f_w = 1 - 0.2\gamma + 9.4\gamma^2 - 19.4\gamma^3 + 27.1\gamma^4 \tag{12}$$

and

$$\gamma = \left(\frac{a}{t}\right)^{\frac{1}{2}} \frac{b}{w}\ , \quad \left(\frac{b}{w} < 0.5\right) \tag{13}$$

Given the global threat of micro-flaws on the stability of large moving systems, understanding detrimental effects of such stress raisers is imperative in the framework of fatigue strength design and risk management. Therefore, through the Sections that follow using the developed computational strategy, the failure resistance of plates with surface flaws was assessed under cyclic loadings.

4. Failure performance evaluations for a surface pre-existing flaw

4.1 Residual life analysis

In Section 1, the strength degradation caused by a semi-elliptical flaw under cyclic loading (Fig. 1) is examined. Notch stress-raiser assessments for the plate made of 7075 T6 aluminium alloy are performed in terms of number of loading cycles, assuming the following material parameters and applied maximum stress: $C_A = C_B = 1.6\ 10^{-10}$, $m_A = m_B = 3.02$, $\beta = 0.7$, $\nu = 0.3$, E = 71.7 GPa, S_{max}= 150 MPa with R= 0.1, whereas initial crack growth lengths in depth and surface (a_0, b_0) directions are reported in Table 1.

Fatigue-induced plate failure is herein examined via a novel damage tolerance-based analytical strategy in order to evaluate the residual life using Eq. (4)-(13) together with Eq. (2) and (3), where the shape effect of semi-elliptical flaw and the stress ratio effect are combined. The evaluated number of loading cycles as a function of crack length is shown in Fig. 2 to Fig. 6 for five different depth-to-length ratios (a_0/b_0 = 0.2, 0.4, 0.6, 0.8, 1.0), respectively. Further, through such Figures and Table 1, the predictive capacity of the obtained estimates is verified employing relevant experimentally tested data discussed by Putra and Schijve [22]. From such comparisons, it can be deduced that the developed computational strategy provides reliable fatigue strength design of plate-type configurations with a semi-elliptical flaw.

In safety-relevant theoretical outcomes generated, a more conservative trend of life estimates for lower depth-to-length ratios is observed. Furthermore, for surface stress raisers from fracture mechanics point of view, it is evident that under cyclic loading due to complex driving force interactions the extension of crack at two critical points does not start simultaneously. Such a phenomenon usually caused by plasticity effects can actually play a significant role in the life resource of component that will be realized and may lead to more conservative assessments in some cases.

It should be also noted that, if the depth-to-length ratio (a_0/b_0 = 0.2) increases three times, the number of loading cycles increases by more than two times whereas, if it increases four times, the life increases about three times. Further, when the ratio is increased by the factor equal to 5, the life increases by more than three times with respect to that evaluated for the relevant depth-to-length ratio and initial crack length in depth direction (i.e. a_0 = 1.92 mm, a_0/b_0 = 0.2).

PLEASE insert Table 1 here.

PLEASE insert Figure 2 here.

PLEASE insert Figure 3 here.

PLEASE insert Figure 4 here.

PLEASE insert Figure 5 here.

PLEASE insert Figure 6 here.

4.2 Driving mode evolutions in the vicinity of the crack tip

4.2.1 Stress intensity factor

Now the stability of the plate with a semi-elliptical flaw (w = 70 mm, t = 8 mm, Fig. 1), made of 7075 T6 aluminum alloy, is assessed via the stress intensity factor. Through such failure evaluations, three initial surface cracks (characterized by the following sizes in depth and surface directions: a_0 = 1.54 mm and b_0 = 7.7 mm, 2.57 mm, 1.54 mm) are analyzed under cyclic loading (S_{max}=120 MPa, R = 0.1).

Disturbed stress state due to pre-existing flaw is herein assessed by means of two fracture mechanics-based computational strategies (i.e. relevant analytical solutions examined in Section 2 and those discussed by Boljanović [19]), taking into account the depth-to-length ratio effect. Evaluated driving intensities for appropriate positions at the crack growth front are listed in Table 2 in the case of three types of surface stress raisers, characterized by a_0/b_0 = 0.2, 0.6 and 1.0, respectively. It is evident that both models provide quite well correlations between different analytical outcomes. It is worth to be also noted that an increase in the depth-to-length ratio from 0.2 to 0.6 (and from 0.6 to 1.0) leads to a decrease in the stress intensity factor by about 23% for the considered semi-elliptical flaws.

4.2.2 Crack growth path

Fatigue degradation analysis presented in this Section is related to the semi-elliptical crack growth path. Damaged plate (w = 100 mm, t = 9.6 mm, Fig. 1) made of 7075 T6 aluminum alloy is subjected to cyclic loading (S_{max}=150 MPa, R = 0.1). The mode intensity analysis is carried out in the case of two different stress raisers whose initial sizes are equal to a_0 = 1.92 mm, b_0 = 2.4 mm (PCA 14) and a_0 = 2.88 mm, b_0 = 7.2 mm (PCA 15) [22] in depth and surface crack growth direction, respectively, employing the same material parameters as those mentioned in Section 4.1.

In the micro-notch analysis, the interaction between the effect of stress raiser and the stress ratio effect is evaluated through novel solutions for crack growth rates in two critical crack growth directions using Eq. (4)-(13) associated with Eq. (1) and (2), respectively. By adopting that the horizontal axis matches with the front face and the vertical axis is normal to the centreline of the plate, analytically evaluated crack growth paths in the case of two initial depth crack sizes (a_0 = 1.92 mm and 2.88 mm, i.e. a_0/b_0= 0.4 and 0.8) are shown in Fig. 7 and 8 for twelve different depth crack lengths, defined through relevant figure captions.

Further, fracture mechanics-based driving mode solutions are verified through the

crack paths experimentally tested by Putra and Schijve [22], as is shown in the same Figures. Thus, it can be deduced that different crack growth paths agree quite well, and relevant effect of depth-to-length ratio coupled with power of stress raiser are adequately generated in the case of semi-elliptical flaws.

PLEASE insert Figure 7 here.

PLEASE insert Figure 8 here.

4.3 Effects of surface flaw shape and thickness on the plate failure

Finally, through the present Section, the strength degradation performance of the cyclically loaded plate (Fig. 1), made of 7075 T6 aluminium alloy, is evaluated taking into account the shape of the pre-existing flaw. The stability of a semi-elliptical crack is assessed here for three different sizes in surface crack growth direction b_0 = 4.25 mm, 6.38 mm, 8.5 mm, a_0 = 3.75 mm associated with plate thickness t = 8 mm, plate width w= 100 mm, and applied maximum force P_{max}= 72000 N with R = 0.2.

Durability of plates with a surface flaw is herein explored in terms of number of loading cycles, involving the depth-to-length ratio effect. Relevant residual life generated for three plates (a_0/b_0 = 0.882, 0.588, 0.441 with a_0 = 3.75 mm) via Eq. (4)-(13) together with Eq. (2) and (3) is shown in Fig. 9(a) and (b) with respect to depth and surface crack direction, respectively. Furthermore, the evaluations for the plates with an initial semi-elliptical flaw (a_0 = 1.55 mm b_0 = 2.43 mm, w = 120 mm, P_{max}= 56100 N, R = 0.1) and three different thicknesses (t = 4.25 mm, 5.95 mm, 7.65 mm) under cyclic loading are examined in Fig. 10(a) and (b) for two critical crack growth directions. Note that failure evaluations are performed by adopting the same material parameters as those discussed in Section 4.1. Additionally, it is evident that, if the depth-to-length ratio decreases, the disturbed stress state of pre-existing flaws (characterized by $a/b \leq 1$) strongly threatens the fatigue performance of plate-type configurations.

PLEASE insert Figure 9 here.

PLEASE insert Figure 10 here.

6. Conclusions

Long-term serviceability of large moving systems is inevitably affected by the presence of a surface stress-raiser, often represented as a semi-elliptical crack-like flaw. Such a deterioration phenomenon caused by manufacturing and/or environmental factors is herein analyzed via novel fracture mechanics-based analytical life solutions, which are successfully assessed through available experimental observations. Further, driving mode interaction in the vicinity of crack tip is theoretically examined taking into account the effect of depth-to-length ratio and the stress ratio effect. Accordingly, the fatigue computational design strategy proposed can help structural engineers and asset managers in making appropriate decisions related to the failure strength resource and structural optimization of safety-relevant plate-type aircraft systems.

Acknowledgement

The present scientific research was supported by the Serbian Ministry of Education, Science and Technological Development through the Mathematical Institute of the Serbian Academy of Sciences and Arts, Belgrade and the COST Association, Brussels, Belgium within the Action CA 18203, which is gratefully acknowledge.

References

[1] R. Jones, D. Peng, S. Pitt, C. Wallbrink, Weight functions, CTOD, and related solutions for cracks at notches, Eng. Failure Anal. 11 (1) (2004) 79-114.

[2] Y. Yamashita, M. Shinozaki, Y. Ueda, K. Sakano, Fatigue crack growth life prediction for surface crack located in stress concentration part based on the three-dimensional finite element method, ASME J. Eng. Gas Turbine Power 126 (2004) 160-166.

[3] N. Antoni, F. Gaisne, Analytical modelling for static stress analysis of pin-loaded lugs with bush fitting, Appl. Math, Model. 35 (1) (2011) 1-21.

[4] S. Mikheevskiy, G. Glinka, D. Algera, Analysis of fatigue crack growth in an attachment lug based on the weight function technique and the UniGrow fatigue crack growth model, Int. J. Fatigue 42 (2012) 88-94.

[5] A.H. Noroozi, G. Glinka, S. Lambert, A study of stress ratio effects on fatigue crack growth using the unified two-parameter fatigue crack growth driving force, Int. J. Fatigue 29 (2007) 1616-1633.

[6] S. Boljanović, S. Maksimović, M. Djurić, Fatigue strength assessment of initial semi-elliptical crack located at a hole, Int. J. Fatigue 92 (2016) 548-556.

[7] D. Kujawski, A new $(\Delta K^{+} K_{max})^{0.5}$ driving force parameter for crack growth in aluminium alloys, Int. J. Fatigue 23 (8) (2001) 733-740.

[8] S. Boljanović, S. Maksimović, A. Carpinteri, B. Jovanović, Computational fatigue analysis of the pin-loaded lug with quarter-elliptical corner crack, Int. J. Appl. Mech. 9 (2017) 1750058.

[9] W. Zhan, N. Lu, C. Zhang, A new approximate model for the *R*-ratio effect on fatigue crack growth rate. Eng. Fract. Mech. 119 (2014) 85-96.

[10] J.C. Newman Jr., E.P. Phillips, M.H. Swain, Fatigue-life prediction methodology using small-crack theory. NASA-TM-110307, National Aeronautics and Space Administration, Langley Research Center, Hampton, Virginia, United States (1997).

[11] X.R. Wu, J.C. Newman, W. Zhao, M.H. Swain, C.F. Ding, E.P. Phillips, Small crack growth and fatigue life predictions for high-strength aluminium alloys part I – experimental and fracture mechanics analysis. Fatigue Fract. Eng. Mater. Struct. 21 (1998) 1289-1306.

[12] S. Boljanović, A. Carpinteri, Modelling the residual strength of fatigue damages at a single semicircular edge notch: Semielliptical crack and through-the-thickness crack, Fatigue Fract. Eng. Mater.Struct. 42 (2019) 1010-1021

[13] X. Huang, T. Moan, Improved modeling of the effect of *R*-ratio on crack growth rate, Int. J. Fatigue 29(4) (2007) 591-602.

[14] A. Carpinteri, Stress-intensity factors for straight-fronted edge cracks in round bars, Eng. Fract. Mech. 42(6) (1992) 1035-1040.

[15] A. Carpinteri, R. Brighenti, S. Vantadori, Notched double-curvature shells with cracks under pulsating internal pressure, Int. J. Press. Vessel Pip. 86(7) (2009) 443-453.

[16] A. Carpinteri, R. Brighenti, S. Vantadori, Influence of the cold-drawing process on fatigue crack growth of a V-notched round bar. Int. J. Fatigue 32(7) (2010) 1136-1145.

[17] Z. He, A. Kotousov, F. Berto, Effect of vertex singularities on stress intensities near plate free surfaces, Fatigue Fract. Eng. Mater. Struct. 38(7) (2015) 860-869.

[18] S. Boljanović, S. Maksimović, Fatigue failure analysis of pin-loaded lugs, Frattura ed Integrità Strutturale 35 (2016) 313-321.

[19] S. Boljanović, Fatigue performance evaluation for crack-like surface flaws, Int. J. Fatigue 124 (2019) 371-379.

[20] J.C. Newman Jr., I.S. Raju, Stress-intensity factor equations for cracks in three-dimensional finite bodies subjected to tension and bending loads, NASA-TM-85793, National Aeronautics and Space Administration, Langley Research Center, Hampton, VA., United States (1984).

[21] A. Carpinteri, Handbook of Fatigue Crack Propagation in Metallic Structures, Amsterdam, Elsevier Science B.V. (1994).

[22] I.S. Putra, J. Schijve, Crack opening stress measurements of surface cracks in 7075-T6 aluminium alloy plate specimen through electron fractography, Fatigue Fract. Eng. Mater. Struct. 15 (4) (1992) 323-338.

FIGURE CAPTIONS

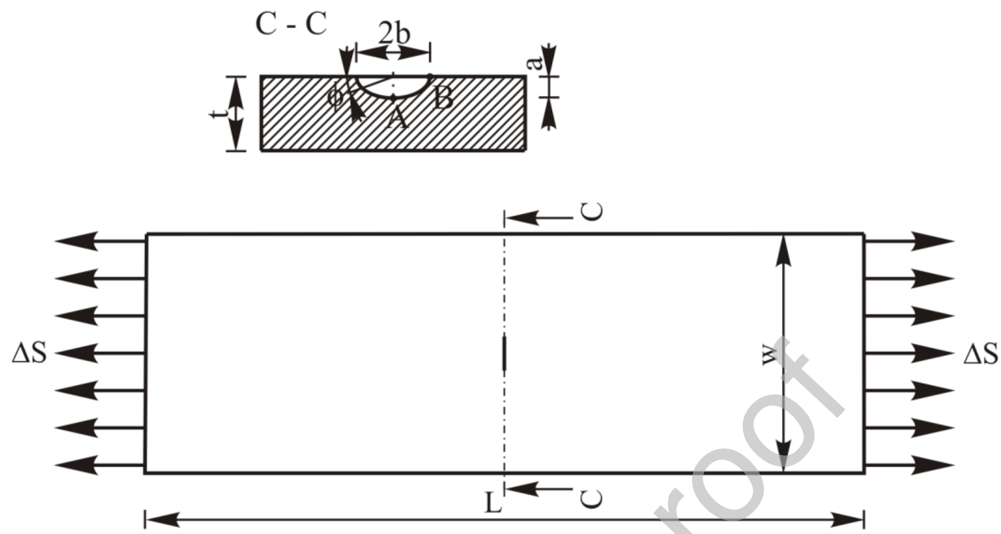

Fig. 1. Cyclically loaded plate with a semielliptical crack-like flaw.

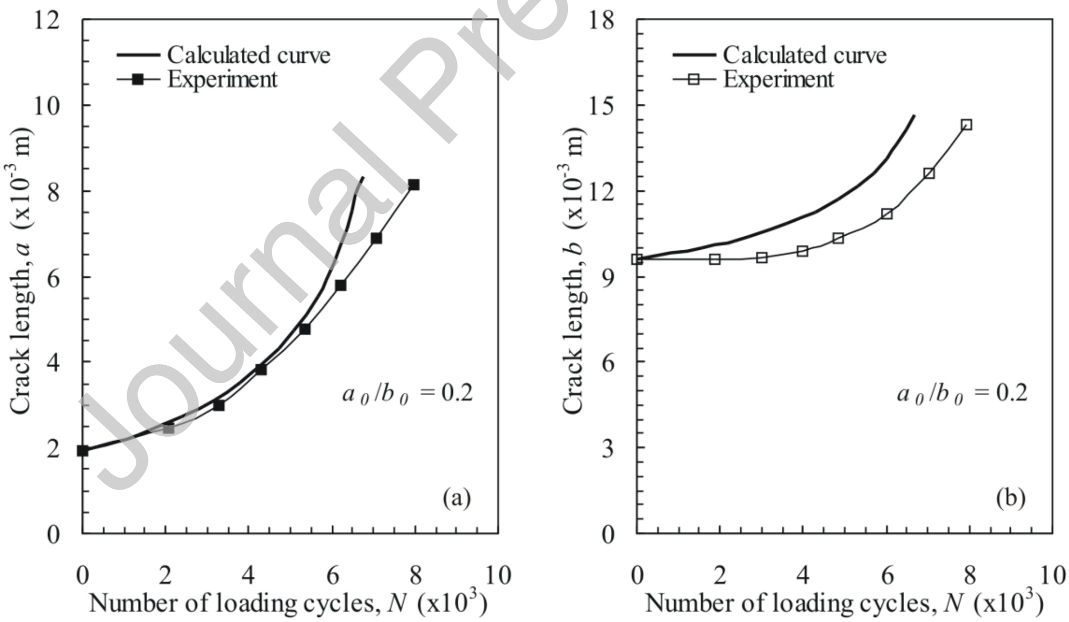

Fig. 2. Fatigue life evaluation for the plate with semi-elliptical flaw: (a) *a* versus *N*, (b) *b* versus *N* (b_0 = 9.6 mm, experiments (PCA6) from Ref. [22] and calculated curves obtained in the present research study).

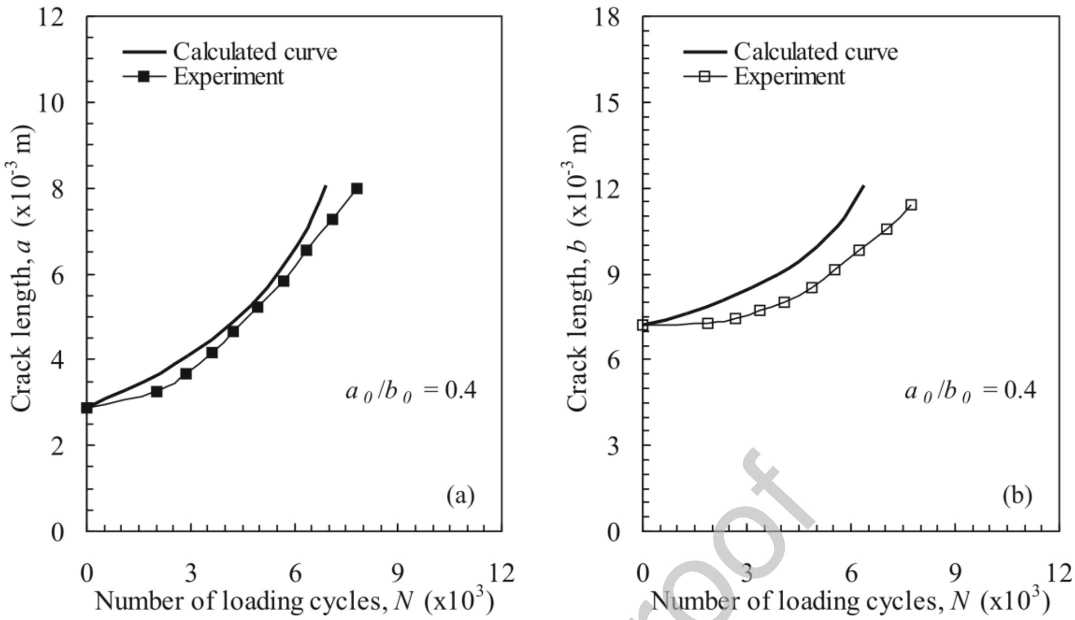

Fig. 3. Fatigue life evaluation for the plate with semi-elliptical flaw: (a) *a* versus *N*, (b) *b* versus *N* (b_0 = 7.2 mm, experiments (PCA15) from Ref. [22] and calculated curves obtained in the present research study).

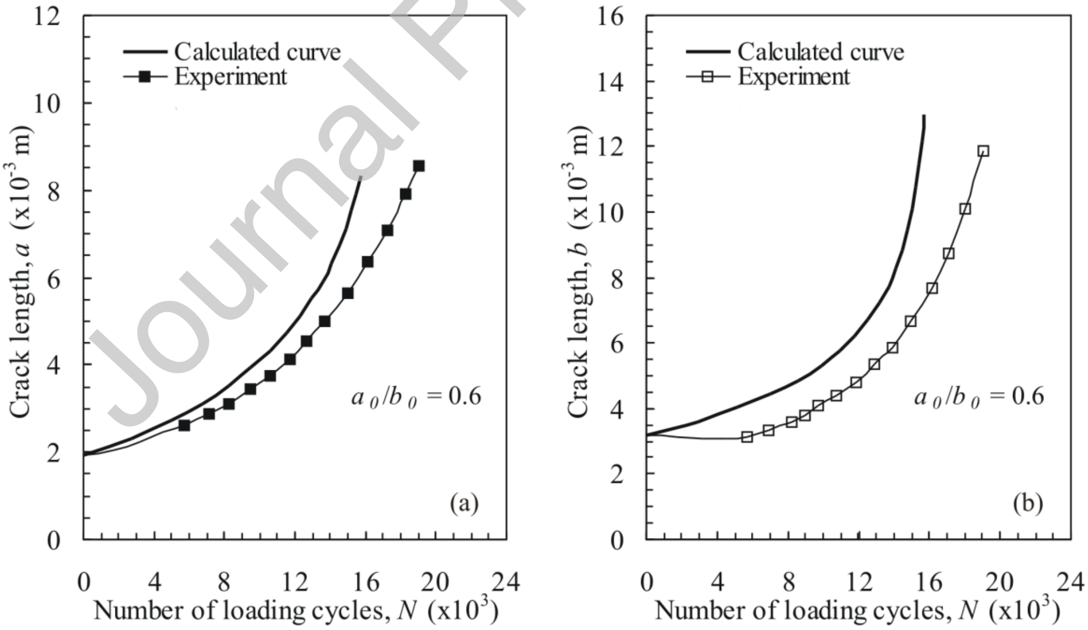

Fig. 4. Fatigue life evaluation for the plate with semi-elliptical flaw: (a) *a* versus *N*, (b) *b* versus *N* (b_0 = 3.2 mm, experiments (PCA2) from Ref. [22] and calculated curves obtained in the present research study).

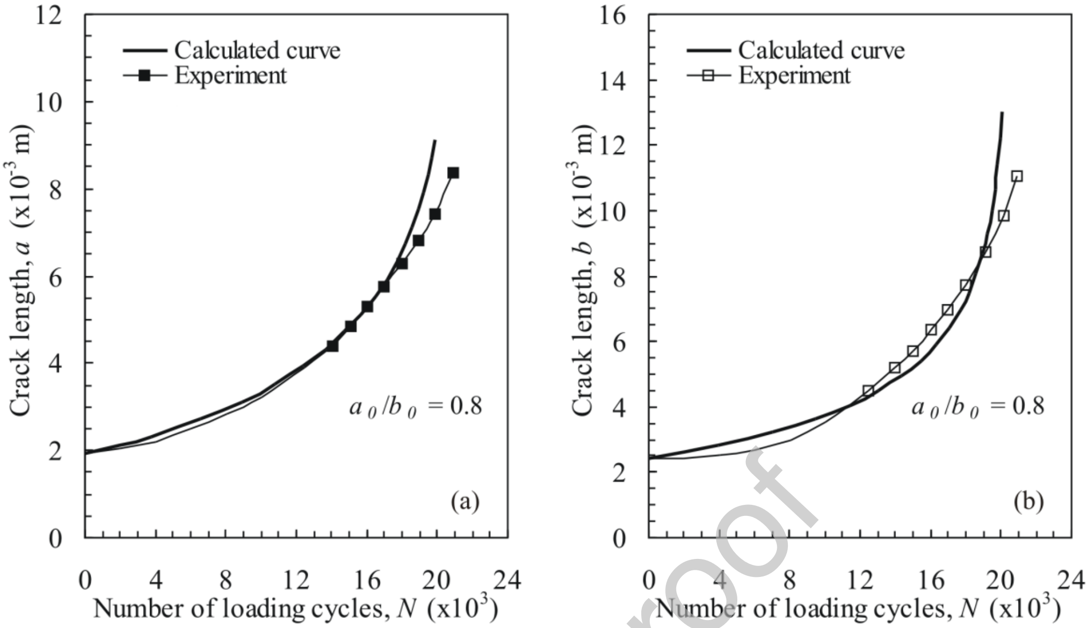

Fig. 5. Fatigue life evaluation for the plate with semi-elliptical flaw: (a) *a* versus *N*, (b) *b* versus *N* (b_0 = 2.4 mm, experiments (PCA14) from Ref. [22] and calculated curves obtained in the present research study).

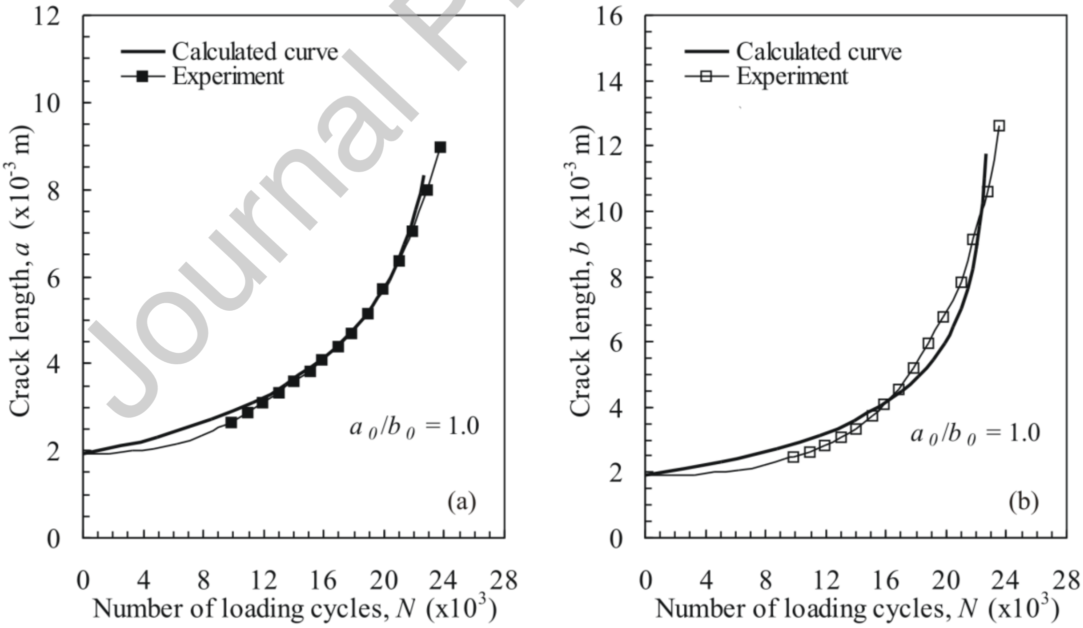

Fig. 6. Fatigue life evaluation for the plate with semi-elliptical flaw: (a) *a* versus *N*, (b) *b* versus *N* (b_0 = 1.92 mm, experiments (PCA13) from Ref. [22] and calculated curves obtained in the present research study).

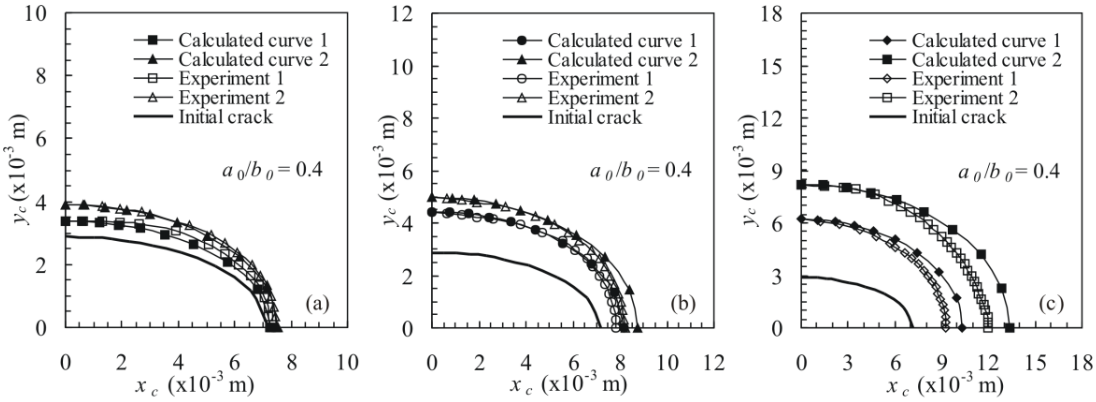

Fig. 7. Crack growth path evolution: (a) 1 - a = 3.38 mm, 2 - a = 3.90 mm, (b) 1 – a = 4.43 mm, 2 – a = 4.97 mm, (c) 1 – a = 6.20 mm, 2 – a = 8.19 mm (a_0/b_0= 0.4, experiments (PCA15) from Ref. [22] and calculated curves obtained within the present research study).

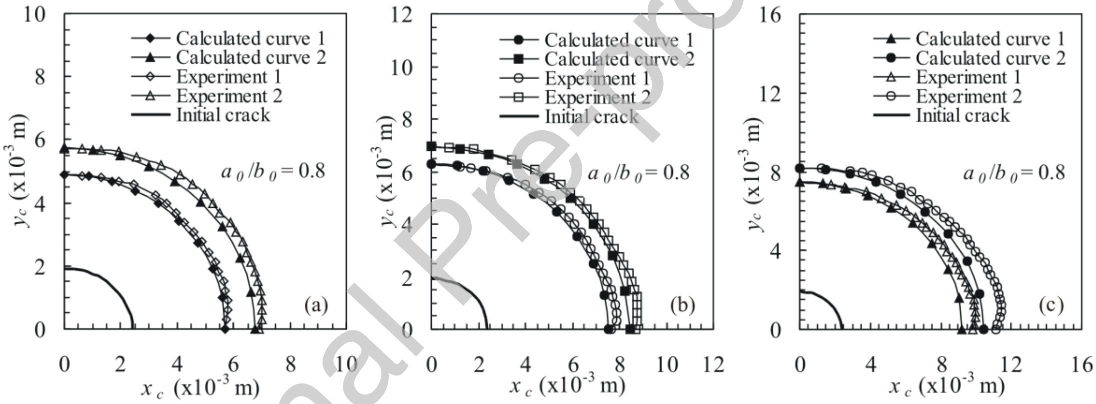

Fig. 8. Crack growth path evolution: (a) 1 – a = 4.89 mm, 2 - a = 5.74 mm, (b) 1 – a = 6.30 mm, 2 – a = 6.95 mm, (c) 1 – a = 7.45 mm, 2 – a = 8.19 mm (a_0/b_0= 0.8, experiments (PCA14) from Ref. [22] and calculated curves obtained within the present research study).

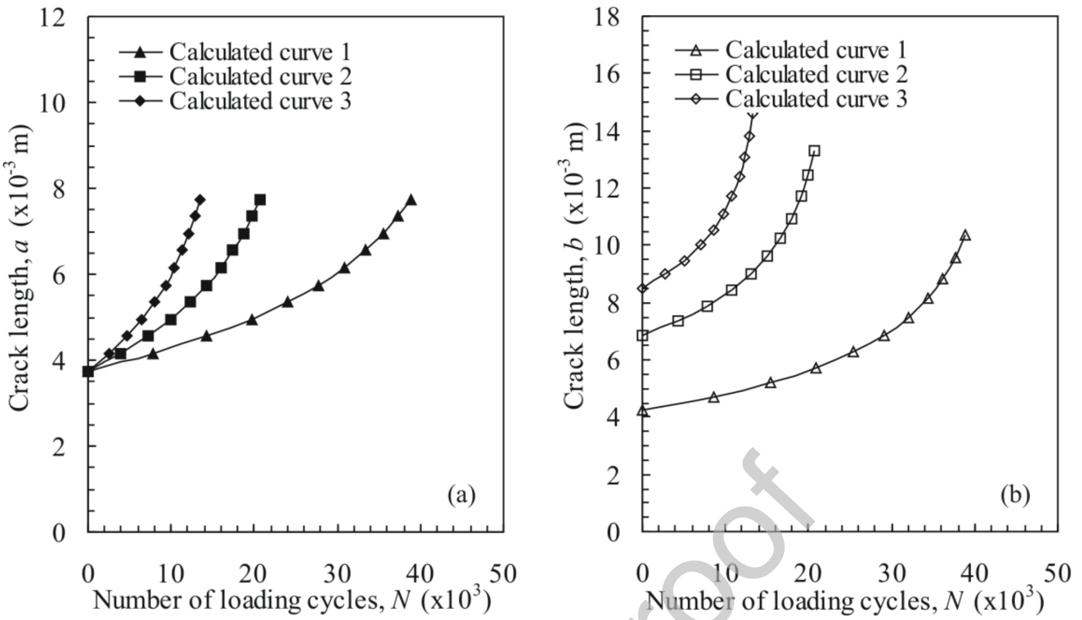

Fig. 9. Fatigue life evaluation for the plate with semi-elliptical flaw (R = 0.2): (a) a versus N, (b) b versus N (1 – b_0 = 4.25 mm, 2 – b_0 = 6.38 mm, 3 – b_0 = 8.5 mm, a_0 = 3.75 mm, calculated curves obtained in the present research study).

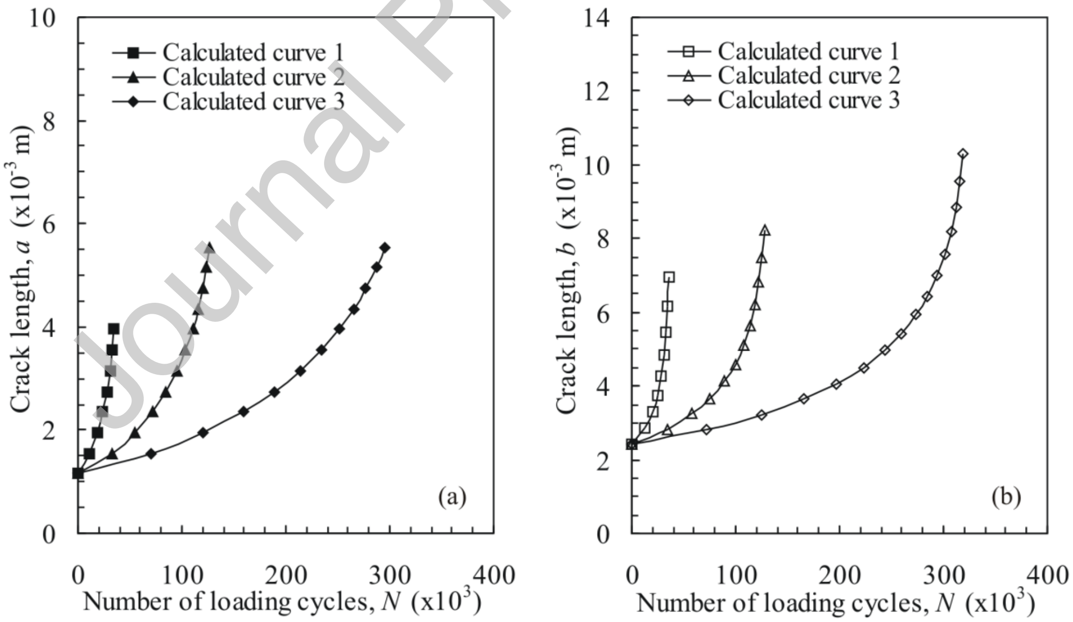

Fig. 10 Fatigue life evaluation for the plate with semi-elliptical flaw (R = 0.1): (a) a versus N, (b) b versus N (1 – t = 4.25 mm, 2 – t = 5.95 mm, 3 – t = 7.65 mm, calculated curves obtained in the present research study).

TABLE CAPTIONS

Table 1. Crack shape parameters and number of loading cycles (experimental data reported in Ref. [22] and calculations obtained within the present research study)

Plate ID [22]	a_0 (mm)	b_0 (mm)	a_0/b_0	$N^{exp.}$ (cycles)	$N^{cal.}$ (cycles)
PCA6	1.92	9.60	0.2	8000	6660
PCA15	2.88	7.20	0.4	8400	6370
PCA2	1.92	3.20	0.6	19000	15680
PCA14	1.92	2.40	0.8	25170	20400
PCA13	1.92	1.92	1.0	24090	22660

Table 2. Stress intensity analysis of a semi-elliptical surface flaw (a_0=1.54 mm) taking into account the effect of depth-to-length ratio.

ϕ (°)	K_{max} (MPam$^{0.5}$)					
	a_0/b_0=0.2		a_0/b_0=0.6		a_0/b_0=1.0	
	Analytical [19]	Analytical	Analytical [19]	Analytical	Analytical [19]	Analytical
0	9.211	9.439	7.010	7.179	5.481	5.572
22.50	8.853	8.846	6.738	6.729	5.268	5.222
45.00	8.550	8.563	6.507	6.513	5.087	5.055
67.50	8.347	8.486	6.353	6.455	4.967	5.010
90	8.276	8.481	6.299	6.451	4.924	5.007